Cellular Signalling 62 (2019) 109332

Contents lists available at ScienceDirect

Cellular Signalling

journal homepage: www.elsevier.com/locate/cellsig

Spatial signal repression as an additional role of Sprouty2 protein variants

Jakob Dittmer, Astrid Stütz, Vanita Vanas, Jihen Salhi, Johannes Manfred Reisecker, Rosana Maria Kral, Hedwig Sutterlüty-Fall*

Institute of Cancer Research, Department of Medicine I, Comprehensive Cancer Center, Medical University of Vienna, Vienna, Austria

ARTICLE INFO

Keywords:
Sprouty2
Spatial signal transduction
MAPK
Phosphorylation variants
Localisation
Nuclear ERK

ABSTRACT

Sprouty2 (Spry2) is a prominent member of a protein family with crucial functions in the modulation of signal transduction. One of its main actions is the repression of mitogen-activated protein kinase (MAPK) pathway in response to growth factor-induced signalling. A common single nucleotide polymorphism within the Spry2 gene creates two protein variants where a proline adjacent to the serine rich domain is converted to an additional serine. Both protein variants perform similar functions although their efficiency in fulfilling these tasks varies. In this report, we used biochemical fractionation methods as well as confocal microscopy to analyse quantitative and qualitative differences in the distribution of Spry2 variants. We found that Spry2 proteins localize not solely to the plasma membrane, but also to other membrane engulfed compartments like for example the Golgi apparatus. In these less dense organelles, predominantly slower migrating forms reside indicating that post-translational modification contributes to the distribution profile of Spry2. However there is no significant difference in the distribution of the two variants. Additionally, we found that Spry2 could be found exclusively in membrane fractions irrespective of the mitogen availability and the phosphorylation status. Considering the interference of extracellular signal-regulated kinase (ERK) activation in the cytoplasm, both Spry2 variants inhibited the levels of phosphorylated ERK (pERK) significantly to a similar extent. In contrast, the induction profiles of pERK levels were completely different in the nuclei. Again, both Spry2 variants diminished the levels of pERK. While the proline variant lowered the activation throughout the observation period, the serine variant failed to interfere with immediate accumulation of nuclear pERK levels, but the signal duration was shortened. Since the extent of the pERK inhibition in the nuclei was drastically more pronounced than in the cytoplasm, we conclude that Spry2 – in addition to its known functions as a repressor of general ERK phosphorylation – functions as a spatial repressor of nucleic ERK activation. Accordingly, a dominant negative version of Spry2 was only able to enhance the pERK levels of serum-deprived cells in the cytosol, while in the nucleus the intensity of the pERK signal in response to serum addition was significantly increased.

1. Introduction

In multicellular organisms, the cellular behaviour is coordinated by intercellular communication. In response to cues in their environment specific cellular responses are stimulated. A complex network of signal transmitters as well as positive and negative regulatory proteins determine signal amplitude and duration and thereby the interpretation of the surrounding information [1].

The members of the Spry protein family are well documented modulators of signal transduction induced by receptor tyrosine kinases (RTK) in response to diverse growth factors [2]. In humans, these proteins interfere with signalling induced by different mitogens primarily of the fibroblast growth factor family, but were also shown to inhibit cellular response to nerve growth factor, vascular endothelial growth factor, platelet-derived growth factor and hepatocyte growth factor [2]. Loss or repression of Spry proteins resembles phenotypes observed in case of growth factor overdoses [3–7]. They fulfil important functions in branching and differentiation processes during development. Accordingly, their deregulated expressions are shown to be involved in tumorigenesis in many organs. For example, Spry2 functions as a tumour suppressor in lung [8,9], prostate [10,11], bone [12], breast [13,14] and liver cancer [15]. An opposing effect is described in

Abbreviations: Sprouty, (Spry); receptor tyrosine kinases, (RTK); mitogen-activated protein kinase, (MAPK); fetal calf serum, (FCS); extracellular signal-regulated kinase 1/2, (ERK1/2); glyceraldehyde 3-phosphate dehydrogenase, (GAPDH)

* Corresponding author at: Institute of Cancer Research, Department of Medicine I, Medical University of Vienna, Borschkegasse 8a, A-1090 Vienna, Austria.
E-mail addresses: jihen.salhi@meduniwien.ac.at (J. Salhi), johannes.reisecker@meduniwien.ac.at (J.M. Reisecker), rosana.kral@boku.ac.at (R.M. Kral), hedwig.sutterluety@meduniwien.ac.at (H. Sutterlüty-Fall).

https://doi.org/10.1016/j.cellsig.2019.05.017
Received 18 March 2019; Received in revised form 29 May 2019; Accepted 29 May 2019
Available online 30 May 2019

colon [16,17] and brain [18], where Spry2 expression enhances malignant transformation processes.

Recent reports additionally attribute an important regulatory role in immunogenic processes to them [19,20].

Since murine Spry proteins are highly expressed where signal induction is observed a negative feedback loop is postulated [21–23]. Accordingly, Spry2 and Spry4 expression are induced in response to growth factor-induced signalling, especially if mitogen-activated protein kinase (MAPK) is activated [24–27]. Furthermore RTK-mediated phosphorylation of tyrosine 55 (Y55) is in combination with palmitoylation [28] considered as an important posttranslational modification triggering the plasma membrane localization of Spry2 [21].

Functionally, Spry2 is shown to interfere with multiple pathways downstream of RTK- induced signalling. In some reports, Spry2 is shown to influence phosphoinositide-3-kinase (PI3K) pathway through phosphatase-and-tensin-homolog (PTEN) [29]. Additionally, it has a negative regulatory function in phospholipase gamma induced pathways [30,31]. Nevertheless, the main pathway Spry2 interferes with is activation of MAPK pathway. Like binding of Growth factor receptor-bound protein2 (Grb2) [25,32] this results in diminished RAS activation. Interaction of Spry proteins with the RAF protein family members inhibits their induction by RAS [33,34] causing the usual observed reduction of extracellular signal-regulated kinase 1/2 (ERK1/2) phosphorylation.

The ERK cascade is an important pathway since > 250 substrates are phosphorylated by this kinase. Although half of the ERK targets including prominent transcription factors like c-Fos, and Elk1 are localized in the nucleus, other substrates in the cytoplasm and in different organelles play important roles in other ERK-induced processes. Therefore, localization of phosphorylated ERK is an important determinant in the signalling response [35,36]. The subcellular origin initiating the RAF-MEK-ERK pathway is crucial in determining the ERK1/2 specificity [37].

In an earlier report, we have investigated the functional consequences of a cytosine to thymidine transition resulting in a substitution of proline for serine at position 106 [38]. This frequent Spry2 variant adds an additional phosphorylation site to the Spry2 protein within the serine rich domain. Serine phosphorylation within this domain was shown to be connected with protein stability [39], this variation is rather modulating the inhibitory potential of Spry2. Although both Spry2 variants affected the malignant processes in order to function as tumour suppressors in lung [8], the efficiency of the inhibition was significantly different [38]. Nonetheless, the potency of their effect on the total ERK1/2 phosphorylation did not always correlate with their influence on the subsequent processes. In this report, we investigated the influence of different Spry2 mutants concerning their localization and their influence on phosphorylated ERK1/2 levels in cytoplasm and nucleus.

2. Material and methods

2.1. Cell culture

The primary embryonic human lung fibroblasts WI-38 were purchased from the American Type Culture Collection. All experiments were performed with cells at passages between 24 and 28. Cells were cultured in a humidified incubator at 37 °C with 7.5% CO_2 in Dulbecco's modified eagle medium supplemented with 10% fetal calf serum (FCS) and penicillin (100 U/ml) as well as streptomycin (100 µg/ml) which was exchanged regularly in intervals of 2–3 days. Serum withdrawal was achieved by washing 50% confluent cell layers twice with serum free medium. 2 days post treatment, cells were infected with the respective adenoviruses and incubated for another 2 days before 20% FCS were added.

2.2. Recombinant adenovirus generation and cell infection

To transiently express proteins in the primary WI-38 cells recombinant replication-deficient adenoviruses were used. The pAdlox constructs were generated earlier as described [8,38]. Recombinant viruses were generated by co-transfecting pAdlox plasmid DNA, digested previously with *Sfi*I, and Ψ5 adenovirus DNA into 293-CRE8 cells as described [40]. Recombinant adenoviruses were selected by serial re-infection of 293-CRE8 cells and amplified in 293 cells, purified by CsCl density-gradient centrifugation, dialyzed against HBS buffer (10 mM HEPES, pH 7.2, 140 mM NaCl, 1 mM $MgCl_2$) and stored at −20 °C. For infection, viruses were diluted in serum-free medium. If not indicated otherwise, adenoviruses were generally used at a multiplicity of infection of 50.

2.3. Sucrose density gradient fractionation

For performing cellular fractionation $1.5*10^7$ cells were washed twice with cold PBS, harvested with cell scrapers, and collected by centrifugation at 1500 rpm for 5 min. The cell pellet was resuspended in 1 ml lysis buffer (250 mM sucrose,10 mM HEPES pH 7.4, 1 mM NaF, 0.5 mM Na_3VO_4) and incubated on ice for 30 min. Lysis was then performed by passing the cell suspension 20 times through a 25G needle. Cell debris and nuclei were removed by a centrifugation step at 1000 *g* and 4 °C for 10 min. 800 µL of the supernatant were loaded onto the prepared sucrose density gradient ranging from 10% to 55% *w/v* (10 layers with decreasing 5% sucrose each step), while the remaining volume was stored at −20 °C and kept as a pre-fractionation control sample (Input). After loading the gradients were centrifuged at 37.000 rpm and 4 °C for 3 h. Thirteen fractions were collected for further analysis.

2.4. Biochemical fractionation using digitonin extraction

Growth medium was discarded and 10^6 cells were washed twice with cold PBS before they were incubated on ice with 0.6 ml cold digitonin solution (40 µg/ml digitonin, 2 mM DTT, 2 mM $MgCl_2$, 1 mM NaF, 0.5 mM Na_3VO_4, 150 mM NaCl, 20 mM HEPES pH 7.4, 200 µM EDTA) for 10 min. Supernatants were then transferred to 1.5 mL microcentrifuge tubes giving rise to the cytosolic fraction and immediately stored at −20 °C until further analysis. Residual cytosolic supernatant was removed by two washing steps with cold PBS. The residual cell fractions were harvested in PBS using cell scrapers and subsequent centrifugation for 5 min at 1000 *g* and 4 °C. The pelleted cells were incubated for 5 min in 150 µL low salt buffer (20 mM HEPES pH 7.4, 0.2 mM EDTA, 1 mM NaF, 0.5 mM Na_3VO_4, 1× complete protease inhibitor), and partly lysed by 15 passages through a 25G needle. To complete lysis, 150 µL high salt buffer (300 mM NaCl, 200 mM HEPES pH 7.4, 0.2 mM EDTA, 1 mM DTT, 1 mM NaF, 0.5 mM Na_3VO_4, 1× complete protease inhibitor) were added and another 15 passages with a 25G syringe needle were performed. Membrane fractions were collected by ultracentrifugation for 30 min at 80.000 g and 4 °C. Supernatant was collected as nucleosol fraction while the pellets (membrane fraction) were washed twice with NEH buffer (150 mM NaCl, 20 mM HEPES pH 7.4, 200 µM EDTA, 1 mM NaF, 0.5 mM Na_3VO_4), resuspended in Laemmli buffer (10% glycerol, 5% β-mercaptoethanol, 2.3% SDS, 65 mM Tris pH 6.8, 0.01% bromophenol blue) and lysed by boiling and sonication.

2.5. Immunoblotting

Immunoblotting was carried out as specified earlier [41] using affinity purified antibodies against Spry2 generated previously [8]. Antibodies against phosphorylated extracellular signal-regulated kinase (pERK) (#9101), and GM130 (#12480) were purchased from Cell Signalling Technology (Danvers, USA) and diluted 1:1000. SP1

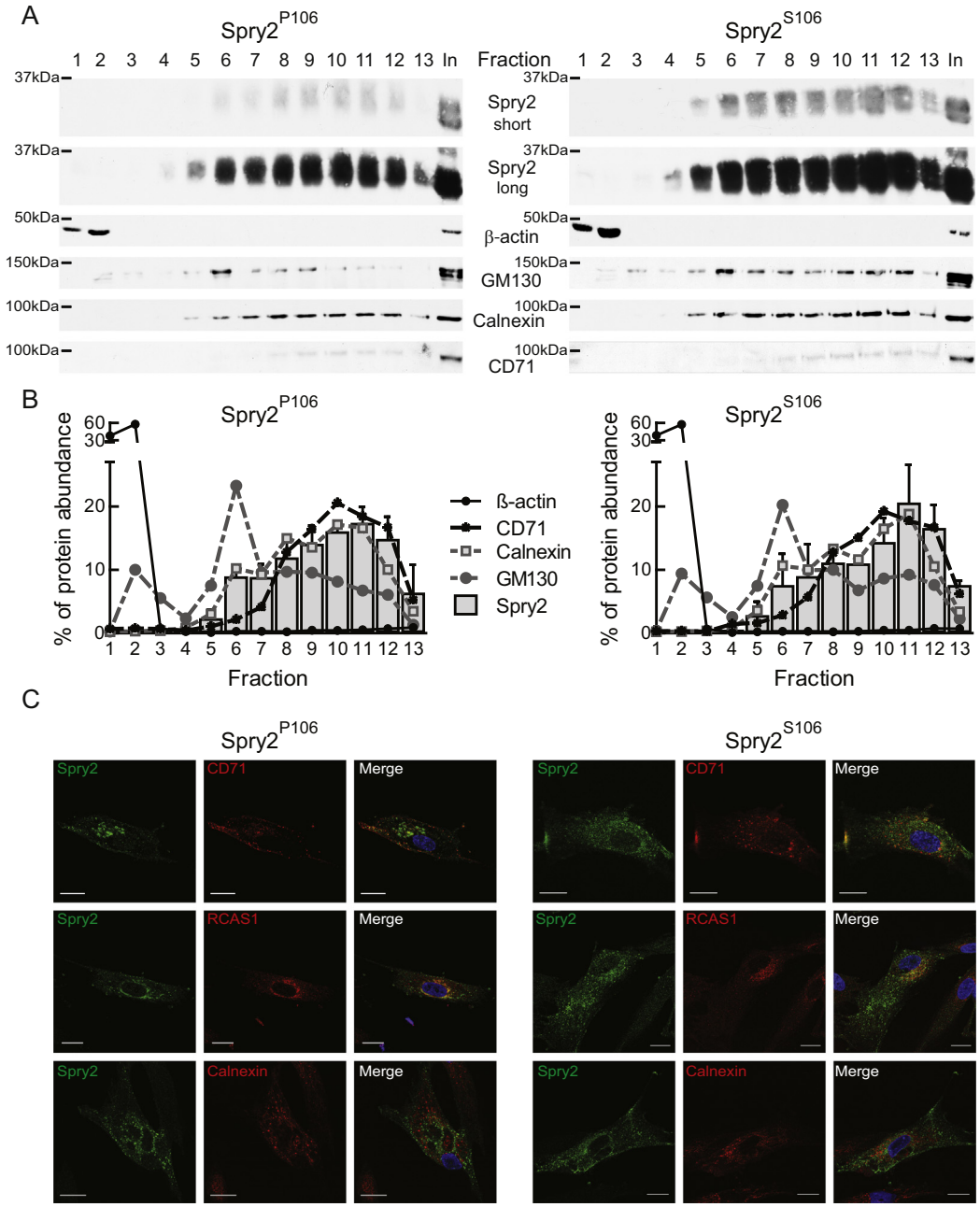

Fig. 1. Localization of the Spry2 variants within the cells. WI-38 cells were serum-starved, infected with either Spry2^{P106} or Spry2^{S106} expressing adenoviruses and serum was added for about 28 h, respectively. (A) Cells were harvested, lysed and a sucrose gradient fractionation was performed and analysed by immunoblot. The harvested 13 fractions were numbered form the top to the bottom and compared with the input (IN). Antibodies specific for Spry2, β-actin, GM130, Calnexin and CD71 were applied. For Spry2 immunoblot short and long exposures are presented as indicated. (B) Protein abundances were calculated after quantification by densitometric analysis using ImageQuant 5.0. Graphs summarize at least three immunoblots and were created using GraphPad prism software. (C) Immunostaining of cells expressing the indicated Spry2 proteins. Localisation of Spry2 was detected with Alexa Fluor 488 in green. Plasma membrane marker CD71, endosomal marker Calnexin and RCAS1 a Golgi specific protein were stained with Alexa Fluor 647 (red). The merged combines the two channels plus the DAPI (Blue) stained nuclei. Bar, 20 μm. (For interpretation of the references to colour in this figure legend, the reader is referred to the web version of this article.)

antibodies (sc-14,027) and antibodies directed against ERK 1/2 (sc-514,302), and CD71 (sc-32,272) were purchased from Santa Cruz (Santa Cruz Biotechnology,Inc., Dallas,Texas) and used in a 1:500 dilution. Antibodies recognizing β-Actin (sc-47,778), and glyceraldehyde 3-phosphate dehydrogenase (GAPDH) (sc-365,062), were also purchased from Santa Cruz (Santa Cruz Biotechnology,Inc., Dallas,Texas) and diluted 1:1000 and 1:3000, respectively. Anti-Calnexin (C4731) antibodies were purchased from Sigma Aldrich (ST. Louis, USA) and applied in a 1: 3000 dilution. The HRP-coupled secondary antibodies were purchased from GE Healthcare (Chalfont St.Giles, UK) and usually incubated in a 1:5000 dilution.

2.6. Immunofluorescence microscopy

WI-38 cells were plated in Eppendorf 8 well imaging cover glass (No. 0030742036). Next day the cells were arrested by serum withdrawal. Another 2 days later the cells were infected with adenoviruses expressing the different Spry2 or control proteins, respectively. Forty-eight hours post-infection cells were stimulated by addition of 20% FCS. For staining cells were rinsed with PBS containing 0.2% BSA and fixed

for 15 min in 4% paraformaldehyde/PBS at room temperature. Fixed cells were washed for 10 min in PBS/100 mM glycine, washed with PBS containing 0.2% BSA and permeabilized in PBS containing 0.2 mg/ml BSA/0.1% Triton X-100/10% Normal Goat Serum (blocking buffer). For dilution of the primary antibodies PBS containing 0.2 mg/ml BSA/0.1%Triton X-100/3% normal goat serum (incubation buffer, or IB) was used. The above mentioned antibodies against Spry2, pERK and CD71 were diluted 1:75, 1:1000, and 1:50, respectively. To stain the Golgi apparatus an antibody against RCAS1 (D8K2E from CST) was diluted 1:50. The endoplasmic reticulum was visualized using the anti-Calnexin antibody (AF18 from Santa Cruz) in a 1:100 dilution. Incubation with the primary antibody was performed overnight at 4 °C in a humidified chamber. Next day, antibodies were removed by three times washing with the PBS/BSA solution. Incubation with the corresponding secondary anti-rabbit and anti-mouse antibodies conjugated to Alexa Fluor 488 or Alexa Fluor 647 was performed for 90 min at room temperature. Both secondary antibodies were diluted 1:1000. The washing step was repeated and DAPI solution (0.2 μg/ml) was added for 15 min. After washing, cells were imaged. Confocal images were obtained using an LSM 880 confocal laser scanning microscope (Carl Zeiss, Inc.) equipped with a 40× Plan-NeoFluar NA 1.3 Oil DIC objective. Images were acquired in three channels: blue (DAPI), green (Alexa Fluor 488), red (Alexa Fluor 647).

3. Results

3.1. Spry2^{P106} and Spry2^{S106} show no difference in their localization

Spry2 protein has three homolog domains which are proposed to impact its function. Beside the frequently studied N-terminal box and Spry-box at the very C-terminus, the serine-rich domain is well conserved. Adjacent to this domain a SNP exchanges the more frequent proline (two third of the alleles) at position 106 to an additional serine [11].

In an earlier study, variation of position 106 in the amino acid sequence of Spry2 was shown to affect the efficiency of Spry2 modes of functions. In the first set of experiments we used biochemical fractionation to analyse if the exchange of proline to a serine at position 106 has an effect on the subcellular localization of Spry2. To obtain a relative synchronized cell population, normal WI-38 cells were serum-deprived and infected with adenoviruses expressing either Spry2^{P106} or Spry2^{S106}, before serum was added for 28 h. Both proteins were primarily detected in the fractions where also CD71 a well-known plasma membrane marker is detected. But Spry proteins appearances were not restricted to the range of CD71-containing fractions but could additionally localize in fractions harbouring Calnexin and GM130, proteins specific for the endoplasmic reticulum and the Golgi apparatus, respectively. Their distribution is not completely overlapping with any of the markers indicating that both Spry2 variants localize to different compartments (Fig. 1A and B). Interestingly, we observed with both variants that in the less dense fractions a slower migrating form is more prominent while in the higher fractions of the gradient slower and faster migrating forms are equally represented (Fig. 1A). Nonetheless, the detected distribution of the two Spry2 variants was almost overlapping, indicating that there is no difference in localization. In line with these data, we could see that a portion of both Spry2 variants resided at the plasma membrane overlapping with regions stained by CD71. Additionally, we observed that Spry2^{P106} as well as Spry2^{S106} were clearly detectable in structures positively highlighted by the Golgi marker RCAS1. In the endoplasmic reticulum stained by Calnexin no significant levels of Spry2 proteins were detected (Fig. 1C). To ensure that the Spry2 variants are equally localized at other phases in the cell cycle, we investigated the distribution of the Spry2 variants within the gradients when serum was added for only 5 h (Fig. 2). As shown earlier [26], at this time point cells are in G1 phase and express Spry2 protein. The distribution of the compartments was slightly different as compared to the pattern observed 28 h after serum addition. Nonetheless, again both Spry2 proteins were found primarily but not exclusively in the fractions harbouring CD71 (Fig. 2A and B). As depicted in Fig. 2C, the endogenous Spry2 levels at these time points are comparable and ectopic expression of both variants causes definitive and equivalent overexpression although to a different extent. These data indicate that both Spry2 variants are distributed similarly to different cellular compartments including plasma membrane and Golgi apparatus.

3.2. In WI-38, Spry2 proteins are exclusively present at membrane structures

Earlier reports show that in serum-deprived transformed monkey (COS1) and in immortalized murine cells, ectopically expressed Spry2 localizes to cytoplasmic structures and undergoes translocation to the plasma membrane only in response to mitogen-activation [42,43]. In order to test if Spry2 shuttles in primary normal human fibroblasts like WI-38 as a consequence of mitogen activation, we serum-deprived cells for 2 days, infected them with adenoviruses expressing either Spry2^{P106} or Spry2^{S106} and isolated the membrane as well as the cytosolic fraction by using digitonin extraction. As depicted in Fig. 3, a cytosolic marker (GAPDH) localized completely to the cytosolic fractions, while markers for the plasma membrane (CD71) and endoplasmic reticulum (Calnexin) were exclusively detected in the membrane fractions. In contrast to the earlier data obtained in other cell systems in starved cells, Spry2^{P106} as well as Spry2^{S106} were undetectable in the cytosolic compartment. In response to serum-induction no changes could be observed.

3.3. Phosphorylation of Y55 is not essential for the localization of Spry2 to the membrane fraction

Since phosphorylation of tyrosine 55 in Spry2 was reported to be essential for the shuttling of Spry2 from the cytoplasm to the plasma membrane, we next investigated the distribution of a Spry2^{Y55F} mutant that cannot be phosphorylated at position 55 and therefore would be expected to reside in the cytoplasm only. Like in the case of the Spry2^{106} variants, also the Spry2^{Y55F} mutant was undetectable in the digitonin extractable cytoplasmic fraction, but present exclusively in the membrane compartments (Fig. 4). Immunoblot with GAPDH proved the successful isolation of a known cytosolic protein. Independent of serum availability, all Spry2 proteins localized to the membrane compartment.

3.4. The influence of Spy2^{S106} on the nuclear pERK levels is clearly distinguishable from the response to Spry2^{P106}

In an earlier report [38], we demonstrated that a Spy2^{S106} variant more effectively inhibits proliferation of WI-38 cells although it is less effective in repressing total ERK phosphorylation. Therefore, we hypothesized that Spry2 could not only inhibit phosphorylation of ERK but also its accumulation in the nuclei. To study this hypothesis, we separated cytosolic and nucleosolic compartments of the cells in response to mitogen activation. As depicted in Fig. 5A, using the applied conditions the cytosol was essentially extracted by digitonin as detected by a GAPDH antibody. In contrast, nucleosolic proteins were restricted to the nuclear compartment as visualized by using the abundant transcription factor SP1 as nucleosolic marker. In a comparison of all three compartments, we observed that Spry2 resides exclusively in membrane fractions while ERK1/2 as well as its phosphorylated forms are predominantly in the cytoplasm. A small proportion of pERK is also detectable in membrane compartments as well as in the nucleosol (Fig. 5B). In accordance with the hypothesis that phosphorylation of ERK is mandatory for its transport into the nucleus, total ERK levels in mitogen-deprived cells can be detected in the cytosol and in the

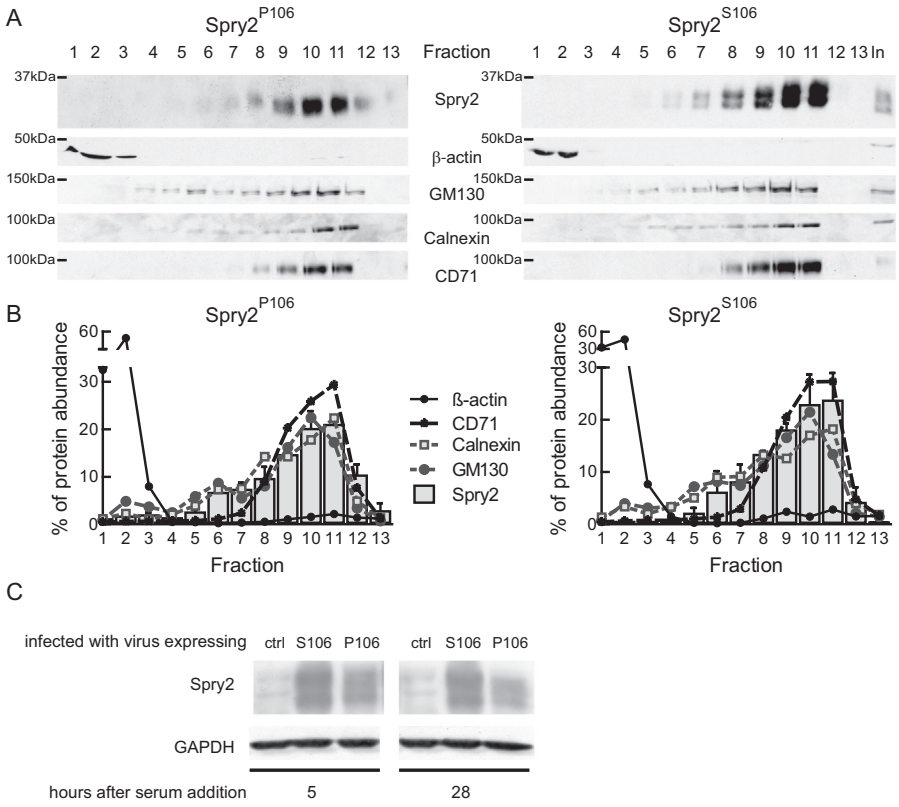

Fig. 2. Localization of the Spry2 in G1 phase cells. Serum-deprived WI-38 cells were infected with the indicated adenoviruses and serum was added for 5 or 28 h, respectively. (A) Five hours after serum addition, a sucrose gradient fractionation was performed and analysed by immunoblot. An immunoblot using antibodies directed against the indicated proteins was performed. (B) Signal intensity of the obtained bands was measured by a densitometric analysis using ImageQuant 5.0. Graphs summarize two to three independent experiments. (C) Part of the infected and serum-induced cells were harvest for comparison of Spry2 expression levels with control-infected cells.

membrane fraction, while in the nucleosol the pattern between ERK and pERK is similar. In serum-deprived cells there is no ERK/pERK in the nucleus and it accumulates after serum application (Fig. 5B). Using digitonin extraction method, we compared the influence of Spry2 protein variants on the cytoplasmic as well as on nuclear pERK levels. As described, cells were serum-deprived and infected with adenoviruses expressing either a control protein (lacZ), Spry2^{P106} or Spry2^{S106}. By adding serum for 5, 10 and 15 min, ERK phosphorylation was induced. While in the cytoplasm, ERK levels were constant within the activation period, phosphorylation of ERK proteins were almost undetectable in serum-deprived cells and in response to mitogen activation pERK levels immediately (5 min time point) accumulated (Fig. 6A and B). In the presence of Spry2, phosphorylation of ERK was also induced in response to serum addition, but the magnitude of induction (as measured after 10 min) was slightly less pronounced (Fig. 6A and B). Nonetheless the cytosolic induction profile of pERK as observed in the presence of Spry2^{P106} was similar to the one measured in the presence of Spry2^{S106}. In the nucleus (Fig. 6C and D), accumulation of phosphorylated ERK in control cells as well as in cells expressing the proline variant was detected throughout the observation period and peaked after 10 to 15 min, but in case of Spry2^{P106}, the induction of nuclear pERK levels in response to serum was on average reduced at all measured time points (Fig. 6C and D). In comparison to the inhibition of pERK levels in the cytoplasm (Fig. 6B), the magnitude of the reduction in the nucleus (Fig. 6C and D) was more pronounced (about half of the levels compared to a 0.8 fold reduction in the cytoplasm). In contrast to cells expressing control or Spry2^{P106} proteins, cells infected with the serine variant of Spry2 showed an immediate increase which was then abrogated to significantly reduced levels after 15 min (0.18 ± 0.08 relative pERK level compared to 0.79 ± 0.09 for control and 0.41 ± 0.03 for Spry2^{P106}, respectively). To verify the observed differences at this time point with another method, we performed an immunostaining using pERK antibodies. Therefore, 2 days serum-starved WI-38 cells were infected with adenoviruses expressing a control protein or one of the Spry2 variants, and then another 2 days later, serum was added for 15 min. In all cells, pERK was easily detectable, although the distributions of the pERK levels were clearly distinguishable. In the control treated cells, most cells were characterized by a very intense pERK staining which typically seemed clearly accumulated in the nucleus. In Spry2^{P106} expressing cells, the staining was frequently less intense, but

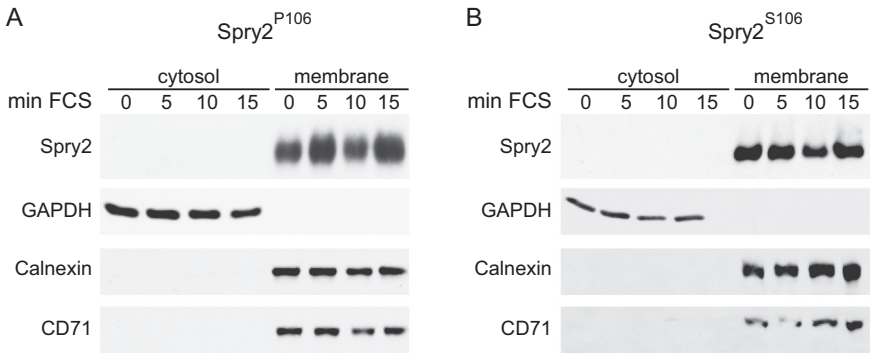

Fig. 3. Spry2^{P106} as well as Spry2^{S106} are exclusively detected at the membrane. Primary lung cells (WI-38) were serum-deprived for 48 h and then infected with adenoviruses expressing either (A) Spry2^{P106} or (B) Spry2^{S106}. Two days later, serum was added to a final concentration of 20% and the digitonin extraction analysis was applied after 0, 5, 10, and 15 min. The cytosolic and membrane fractions were analysed by subsequently applying the indicated antibodies in an immunoblot, respectively. A representative picture of at least three experiments is shown.

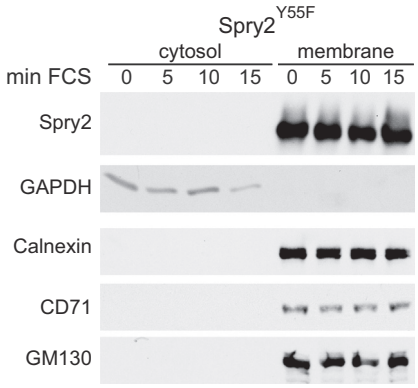

Fig. 4. Dominant negative Spry2^{Y55F} localizes to the membrane independent of serum availability. Cells were infected with adenoviruses expressing Spry2^{Y55F} two days after serum-deprivation. Two days later, FCS was added for the indicated times. Cells were lysed and fractionated by digitonin extraction and an immunoblot was performed. Representative images of the cytosolic and membrane fractions after the application of Spry2, GAPDH, Calnexin, CD71 and GM130 antibodies are depicted.

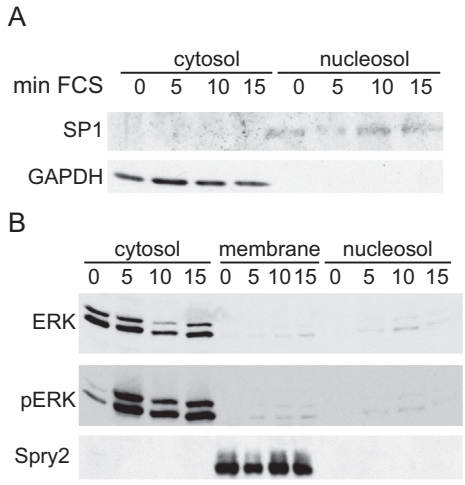

Fig. 5. Fractionation of cells using digitonin extraction and consecutive ultracentrifugation. WI-38 cells were serum deprived and infected with control adenoviruses expressing Spry2. 4 days after serum removal, 20% FCS was added for different timespans. After 0, 5, 10 and 15 min, cytosol was extracted by digitonin and membrane enclosing structures were removed by ultracentrifugation. (A) The received cytosol and nucleosol were analysed by immunoblot with the indicated antibodies and a representative picture is shown. (B) Fractions containing cytosol, membrane compartments (membrane) and nucleosol were compared concerning their ERK, pERK and Spry2 levels.

there was still a slight enrichment of pERK in the nucleus, while in the cells with an ectopically introduced serine variant of Spry2, no accumulation of pERK in the nucleus was observed. (Fig. 6E). These data indicate that Spry2 inhibits not only the phosphorylation of ERK but also its accumulation in the nucleus.

3.5. The dominant negative effect of the Y55F Spry2 mutant on pERK levels in cytoplasm and nucleus is different

In some reports, phosphorylation of tyrosine (Y) 55 in Spry2 is shown to be critical for its function [43]. Introduction of a phenylalanine (F) at this position mimics an unphosphorylated form which can function as a dominant-negative or negative Spry2 version. Therefore, we tested the influence of Spry2^{Y55F} mutant expression on ERK phosphorylation and its translocation into the nucleus. As shown in Fig. 7A, expression of this mutant has a strong influence on pERK levels in arrested cells. Unlike in control treated cells as well as in WI-38 fibroblasts expressing Spry2^{P106} or Spry2^{S106} (compare Fig. 6), a significant amount of ERK proteins is phosphorylated even in serum-deprived cells substantiating the dominant-negative effect of this variant (Fig. 7B). In response to serum addition, however, the immediate increase of phosphorylated ERK is less pronounced than in control cells (Fig. 7A and B). Interestingly, the nuclear pERK levels in serum-deprived cells are not influenced by the Spry2^{Y55F} expression, but after addition of serum pERK is more effectively translocated to the nucleus than in the control cells (Fig. 7C and D), indicating that the lack of the tyrosine at position 55 is also dominant negative with regard to the Spry2 effect on inhibition of nuclear accumulation of pERK. Corroborating, in most serum-starved cells expressing Spry2^{Y55F}, pERK staining was more abundant than in the control cells although it was mainly in the cytoplasm. After serum induction of the cells, the pERK concentration in the nuclei of Spry2^{Y55F} expressing cells was in fact more demonstrative than in control cells. These observations substantiate that Spry2 influences distribution of pERK to the nucleus.

4. Discussion

The cellular response to multiple environmental signals is a strictly coordinated process. Many canonical and non-canonical signal transduction pathways are integrated in this network. One of the most prominent and important activation cascades involves MAPK pathways and its multiple substrates [36]. Temporal and spatial fine tuning of signal intensities affects the outcome at the end of the cascade since even opposing processes like differentiation and proliferation can be initiated [35,44]. Deregulation of this pathway has a well-documented impact in the development of cancer but is also shown to contribute in neurodegenerative and cardiovascular diseases [45].

Spry2 belongs to a family of proteins which is crucially involved in the modulation of signal duration and maybe also intensity in response to RTK-mediated signalling [46]. Although it functions in different pathways Spry2 is mainly shown to interfere with MAPK signalling.

Two major variants of the protein in have been described in healthy human beings. A cytosine to thymidine transition in the nucleic acid sequence results in a conversion of a proline to a serine at position 106. Both proteins are shown to influence cell proliferation, migration and adhesion of cells although to different efficiency [38]. Since the effectiveness of the variants in their ability to interfere with ERK phosphorylation fails to reflect their potency in migratory and proliferation processes, in this study we focused on spatial differences of the two variants.

We found that both variants were exclusively present in membrane fractions irrespective of the availability of mitogens. In an earlier report using COS-1 cells, in the absence of mitogen Spry2 was shown to localize in the cytoplasm but changed its localization to the plasma membrane in response to growth factor addition. C-terminal sequences were important to confer this translocation [42]. Comparable observations were documented by Mason et al., in NIH3T3 cells Spry2 changed its localization in response to epidermal growth factor (EGF), although the protein was always associated with some membrane engulfed structures [43]. Additionally, one report suggests the possibility that Spry2 forms huge aggregates [47]. Since in our study, size of the structures was a determining fractionation factor we are not able to exclude that Spry2 is associated to a high molecular structure free of a membrane envelope.

Furthermore, we observed that in a sucrose gradient, Spry2 protein is not solely associated with the plasma membrane fractions. A proportion of the protein rather appears to be also associated with the endoplasmic reticulum or Golgi apparatus. This supports earlier observations, showing that Spry2 localizes to endosomes to fulfil functions in regulation of EGFR signalling [48]. Spry2 distribution is not influenced by the variation at codon 106, although with the Spry2^{S106} it becomes more obvious that a posttranslational event is involved in the

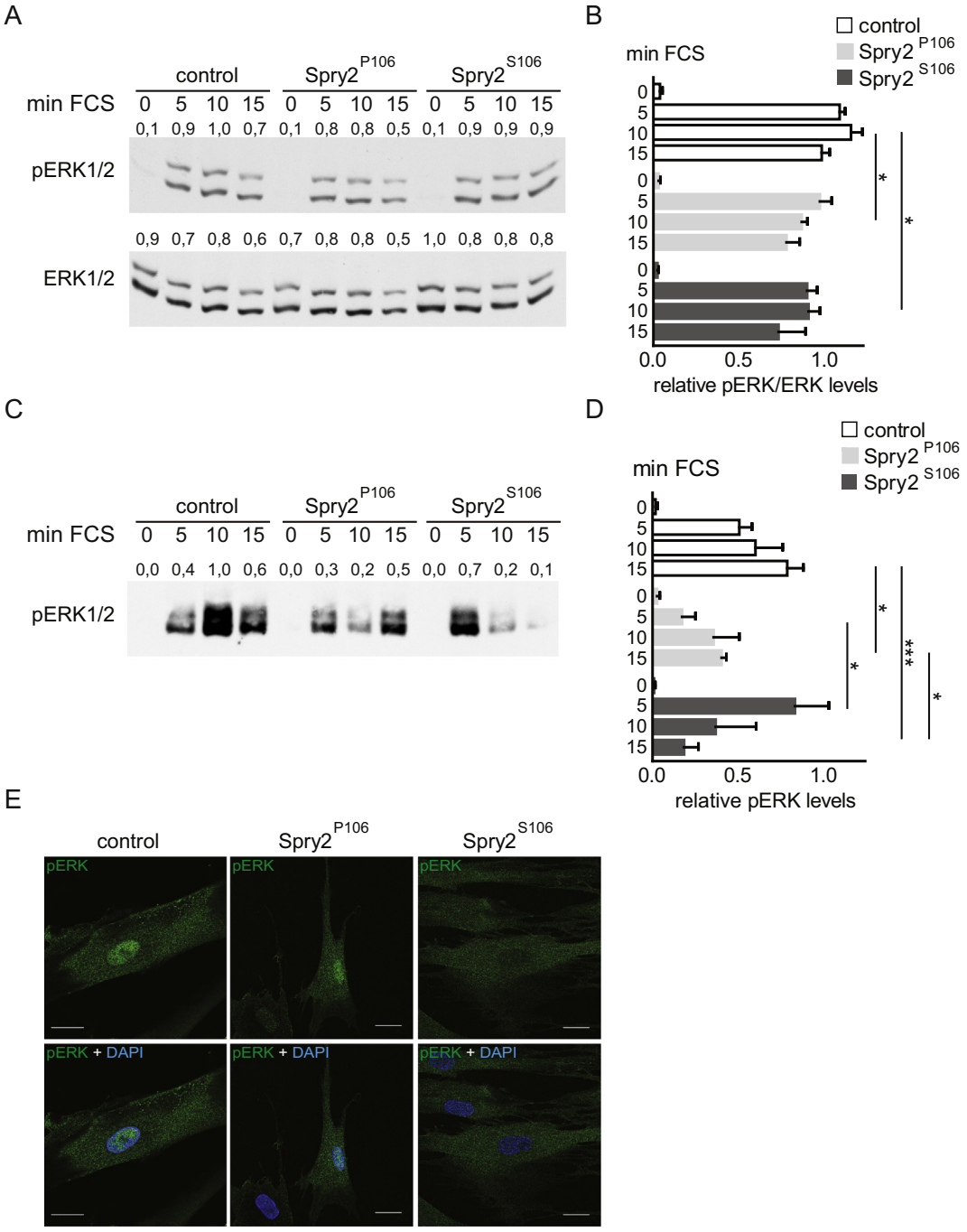

Fig. 6. Influence of Spry2 codon 106 variants on ERK activation in different compartments after serum addition. Primary cells (WI-38) were serum-starved for 48 h and then infected with adenoviruses expressing either a control protein (lacZ), Spry2^{P106} or Spry2^{S106}. Two days later, cells were incubated with serum for the indicated times. (A) Representative immunoblots from the cytosolic fraction of an experiment using antibodies recognizing pERK1/2 and total ERK1/2 are shown. Using ImageQuant 5.0, the pERK1/2 bands detected in response to serum addition were quantified and normalized to the corresponding values obtained for the ERK expression. The highest values within the control treated group were arbitrarily set as 1. The numbers of the presented blots are shown (B) A summary of calculated mean values ± SEM from four to five experiments is depicted. Significance between the three groups was calculated by using a 1Way ANOVA-test in GraphPad prism. *$p < .05$; (C) In parallel the nucleosolic fractions were analysed using pERK antibodies. (D) The bands were densitometrically quantified using ImageQuant 5.0, and the highest values of each experiment were set as 1. The graph summarizes 4 to 5 experiments. Significance was determined by 1Way ANOVA-test in using GraphPad prism software. *p < .05; ***$p < .001$. (E) Immunofluorescence of cells expressing the indicated proteins were performed after a 15 min stimulation period. Localisation of pERK was detected with Alexa Fluor 488 in green. A picture representing the majority of cells is shown. The merged image combines the pERK staining (green) with the DAPI (Blue) stained nuclei. Bar, 20 µm. (For interpretation of the references to colour in this figure legend, the reader is referred to the web version of this article.)

localization to this compartment. Accordingly, in the report of Mason et al., EGF caused tyrosine phosphorylation of Spry2 at Y55 and other tyrosine residues and this additional tyrosine phosphorylation events were responsible for the delocalization from the plasma membrane fraction [43].

Although the localization of the Spry2 variants is not obviously different, their influence on MAPK activation is clearly distinguishable. While Spry2^{P106} is mainly reducing the intensity of the pERK signal, the

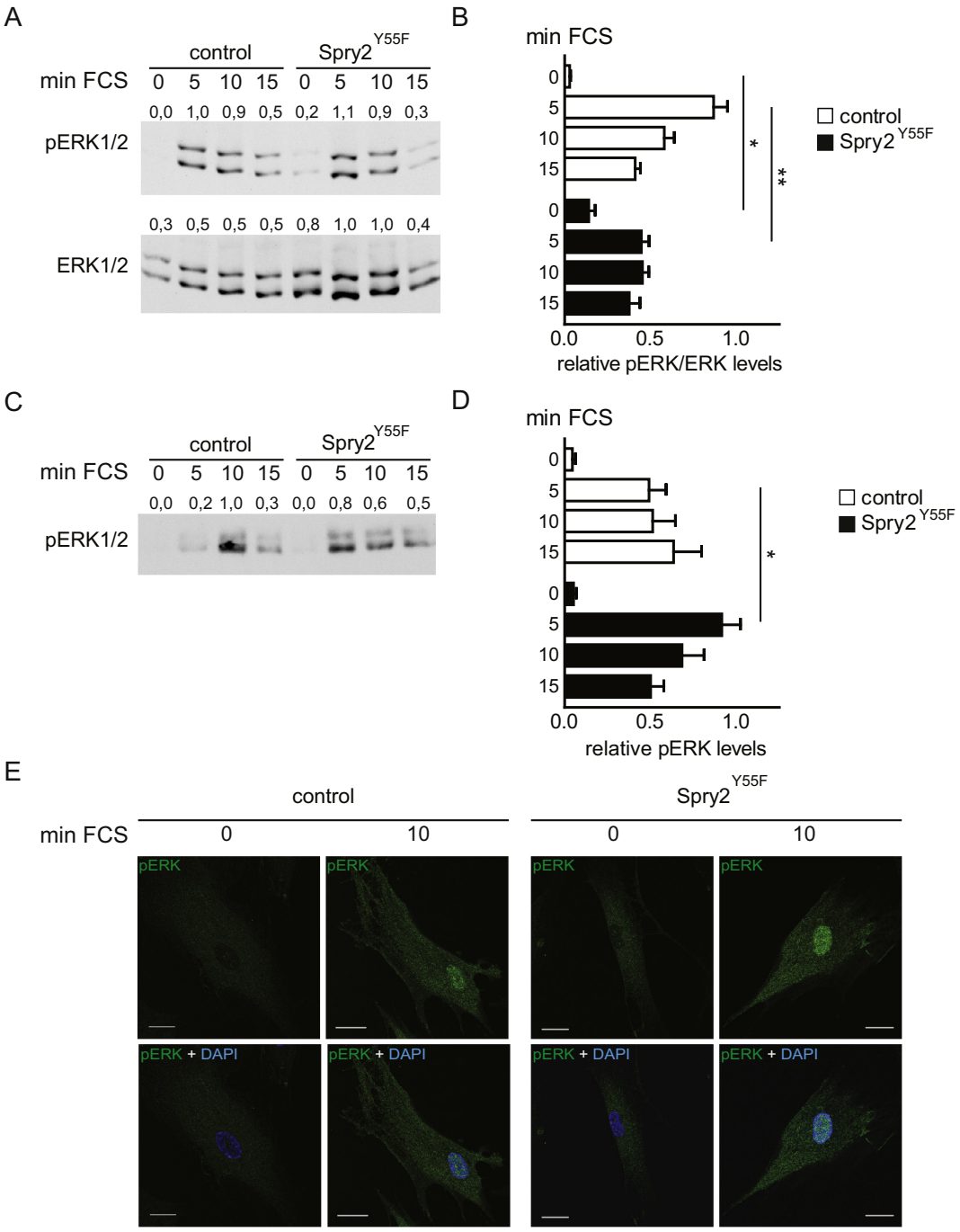

Fig. 7. : Influence of the dominant-negative Spry2^{Y55F} mutant on pERK levels in different compartments of the cell. Serum-starved WI-38 cells were infected with adenoviruses expressing Spry2^{Y55F} or a control virus. 48 h postinfection, signalling was activated by adding serum for the indicated times and digitonin fractionation was applied. (A) pERK1/2 and total ERK1/2 were detected in the cytosolic fractions by using immunoblotting. The blots of a representative experiments are pictured and the levels determined by densitometric analysis with ImageQuant 5.0. The highest values within the control treated group were arbitrarily set as 1. (B) Mean values ± SEM from five experiments are depicted. Significance was calculated by using an unpaired *t*-test. *p < .05; **p < .01 (C) pERK levels in the corresponding nucleosolic fractions are shown. To quantify the levels, band intensities were compared using ImageQuant 5.0 and the highest value in the control group was arbitrarily set as 1. (D) The calculated pERK levels of 5 experiments are summarized and the significant difference is indicated. *p < .05; (E) Serum starved cells expressing either a control protein or the Spry2^{Y55F} mutant were serum-stimulated for the indicated times. Images of pERK were acquired using a LSM 880 confocal microscope. A representative image of each time point is depicted. The merged images show pERK (green) and DAPI (Blue) stainings. Bar, 20 µm.

expression of Spry2^{S106} is primarily shortening the duration of signalling. However, both variants are more efficiently repressing pERK levels in the nucleus than in the cytoplasm indicating an additional Spry2 function. In corroboration with this conclusion, expression of the dominant negative form of Spry2^{Y55} boosts the pERK signalling in the nucleus after addition of serum, while in the cytoplasm the pERK intensity is mainly elevated in serum-arrested cells. The mechanism behind this additional Spry2 function is unclear. It is conceivable that Spry2 is directly influencing the transport of proteins, since in earlier reports it was shown to interact with components of intracellular trafficking like hepatocyte growth factor-regulated tyrosine kinase substrate (Hrs) [48] and with EAP20 a protein of the ESCRIT II complex,

also involved in transporting protein within the endosomal compartments [49]. Furthermore, it is possible that some phosphatases Spry2 interacts with are more effective dephosphorylating pERK in the nucleus than in the cytoplasm. Sustained ERK phosphorylation as a result of phosphatase binding was shown as the mode of action for the protein Mxi2 [50], but the phosphatases Spry2 is shown to interact with are not primarily nuclear e.g. PP2A [51], MKP1 or MKP5 [52]. Since the subcellular place from which ERK is induced is critical concerning its substrate specificity, we could also speculate that Spry2 is interfering with compartment specific pERK activation which in consequence would result in a more intense suppression of nuclear pERK levels. Up to now, only Spry4 has been shown to specifically reduce signalling from the ER but not from the plasma membrane [53].

5. Conclusion

Taken together, our data document that Spry2 interferes with pERK activation in the cytoplasm less effective than in the nucleus indicating a new role of Spry2 in propagation of pERK signalling into the nucleus and thereby functioning as a spatial repressor.

Acknowledgements

This work was supported by the Herzfelder'sche Familienstiftung. We thank Sandra Neubauer for her assistance.

References

[1] I. Dikic, S. Giordano, Curr. Opin. Cell Biol. 15 (2003) 128–135.
[2] S. Masoumi-Moghaddam, A. Amini, D.L. Morris, Cancer Metastasis Rev. 33 (2014) 695–720, https://doi.org/10.1007/s10555-014-9497-1.
[3] M.A. Basson, S. Akbulut, J. Watson-Johnson, R. Simon, T.J. Carroll, R. Shakya, I. Gross, G.R. Martin, T. Lufkin, A.P. McMahon, P.D. Wilson, F.D. Costantini, I.J. Mason, J.D. Licht, Dev. Cell 8 (2005) 229–239.
[4] M.A. Basson, J. Watson-Johnson, R. Shakya, S. Akbulut, D. Hyink, F.D. Costantini, P.D. Wilson, I.J. Mason, J.D. Licht, Dev. Biol. 299 (2006) 466–477.
[5] K. Shim, G. Minowada, D.E. Coling, G.R. Martin, Dev. Cell 8 (2005) 553–564.
[6] T. Taketomi, D. Yoshiga, K. Taniguchi, T. Kobayashi, A. Nonami, R. Kato, M. Sasaki, A. Sasaki, H. Ishibashi, M. Moriyama, K. Nakamura, J. Nishimura, A. Yoshimura, Nat. Neurosci. 8 (2005) 855–857.
[7] K. Taniguchi, T. Ayada, K. Ichiyama, R. Kohno, Y. Yonemitsu, Y. Minami, A. Kikuchi, Y. Maehara, A. Yoshimura, Biochem. Biophys. Res. Commun. 352 (2007) 896–902.
[8] H. Sutterluty, C.E. Mayer, U. Setinek, J. Attems, S. Ovtcharov, M. Mikula, W. Mikulits, M. Micksche, W. Berger, Mol. Cancer Res. 5 (2007) 509–520.
[9] A.T. Shaw, A. Meissner, J.A. Dowdle, D. Crowley, M. Magendantz, C. Ouyang, T. Parisi, J. Rajagopal, L.J. Blank, R.T. Bronson, J.R. Stone, D.A. Tuveson, R. Jaenisch, T. Jacks, Genes Dev. 21 (2007) 694–707.
[10] J.L. Schutzman, G.R. Martin, Proc. Natl. Acad. Sci. U. S. A. 109 (2012) 20023–20028, https://doi.org/10.1073/pnas.1217204109.
[11] A.B. McKie, D.A. Douglas, S. Olijslagers, J. Graham, M.M. Omar, R. Heer, V.J. Gnanapragasam, C.N. Robson, H.Y. Leung, Oncogene. 24 (2005) 2166–2174, https://doi.org/10.1038/sj.onc.1208371.
[12] N. Rathmanner, B. Haigl, V. Vanas, A. Doriguzzi, A. Gsur, H. Sutterluty-Fall, FEBS Lett. 587 (2014) 2597–2605.
[13] V. Vanas, E. Muhlbacher, R. Kral, H. Sutterluty-Fall, Tumour Biol. 35 (2014) 4447–4456.
[14] T.L. Lo, P. Yusoff, C.W. Fong, K. Guo, B.J. McCaw, W.A. Phillips, H. Yang, E.S. Wong, H.F. Leong, Q. Zeng, T.C. Putti, G.R. Guy, Cancer Res. 64 (2004) 6127–6136.
[15] C.W. Fong, M.S. Chua, A.B. McKie, S.H. Ling, V. Mason, R. Li, P. Yusoff, T.L. Lo, H.Y. Leung, S.K. So, G.R. Guy, Cancer Res. 66 (2006) 2048–2058, https://doi.org/10.1158/0008-5472.CAN-05-1072.
[16] C. Holgren, U. Dougherty, F. Edwin, D. Cerasi, I. Taylor, A. Fichera, L. Joseph, M. Bissonnette, S. Khare, Oncogene. 29 (2010) 5241–5253.
[17] A. Barbachano, P. Ordonez-Moran, J.M. Garcia, A. Sanchez, F. Pereira, M.J. Larriba, N. Martinez, J. Hernandez, S. Landolfi, F. Bonilla, H.G. Palmer, J.M. Rojas, A. Munoz, Oncogene. 29 (2011) 4800–4813.
[18] J.W. Park, G. Wollmann, C. Urbiola, B. Fogli, T. Florio, S. Geley, L. Klimaschewski, Neuro-Oncology 20 (2018) 1044–1054, https://doi.org/10.1093/neuonc/noy028.
[19] S. Collins, A. Waickman, A. Basson, A. Kupfer, J.D. Licht, M.R. Horton, J.D. Powell, PLoS One 7 (2012) e49801, , https://doi.org/10.1371/journal.pone.0049801.
[20] H.M. Shehata, S. Khan, E. Chen, P.E. Fields, R.A. Flavell, S. Sanjabi, Proc. Natl. Acad. Sci. U. S. A. 115 (2018) E8939–E8947, https://doi.org/10.1073/pnas.1808320115.
[21] D. Chambers, I. Mason, Mech. Dev. 91 (2000) 361–364.
[22] O.D. Klein, G. Minowada, R. Peterkova, A. Kangas, B.D. Yu, H. Lesot, M. Peterka, J. Jernvall, G.R. Martin, Dev. Cell 11 (2006) 181–190.
[23] G. Minowada, L.A. Jarvis, C.L. Chi, A. Neubuser, X. Sun, N. Hacohen, M.A. Krasnow, G.R. Martin, Development. 126 (1999) 4465.
[24] A. Doriguzzi, B. Haigl, A. Gsur, H. Sutterluty-Fall, Int. J. Biochem. Cell Biol. 64 (2015) 220–228, https://doi.org/10.1016/j.biocel.2015.04.017.
[25] I. Gross, B. Bassit, M. Benezra, J.D. Licht, J. Biol. Chem. 276 (2001) 46460–46468.
[26] C.E. Mayer, B. Haigl, F. Jantscher, G. Siegwart, M. Grusch, W. Berger, H. Sutterluty, Cell. Mol. Life Sci. 67 (2010) 3299–3311, https://doi.org/10.1007/s00018-010-0379-6.
[27] K. Ozaki, R. Kadomoto, K. Asato, S. Tanimura, N. Itoh, M. Kohno, Biochem. Biophys. Res. Commun. 285 (2001) 1084–1088, https://doi.org/10.1006/bbrc.2001.5295.
[28] M.A. Impagnatiello, S. Weitzer, G. Gannon, A. Compagni, M. Cotten, G. Christofori, J. Cell Biol. 152 (2001) 1087–1098.
[29] F. Edwin, R. Singh, R. Endersby, S.J. Baker, T.B. Patel, J. Biol. Chem. 281 (2006) 4816–4822.
[30] S. Akbulut, A.L. Reddi, P. Aggarwal, C. Ambardekar, B. Canciani, M.K. Kim, L. Hix, T. Vilimas, J. Mason, M.A. Basson, M. Lovatt, J. Powell, S. Collins, S. Quatela, M. Phillips, J.D. Licht, Mol. Biol. Cell 21 (2010) 3487–3496.
[31] S.Y. Chow, C.Y. Yu, G.R. Guy, J. Biol. Chem. 284 (2009) 19623–19636.
[32] H. Hanafusa, S. Torii, T. Yasunaga, E. Nishida, Nat. Cell Biol. 4 (2002) 850–858.
[33] A. Sasaki, T. Taketomi, R. Kato, K. Saeki, A. Nonami, M. Sasaki, M. Kuriyama, N. Saito, M. Shibuya, A. Yoshimura, Nat. Cell Biol. 5 (2003) 427–432.
[34] P. Yusoff, D.H. Lao, S.H. Ong, E.S. Wong, J. Lim, T.L. Lo, H.F. Leong, C.W. Fong, G.R. Guy, J. Biol. Chem. 277 (2002) 3195–3201.
[35] B. Casar, A. Pinto, P. Crespo, Cell Cycle 8 (2009) 1007–1013, https://doi.org/10.4161/cc.8.7.8078.
[36] E. Wainstein, R. Seger, Curr. Opin. Cell Biol. 39 (2016) 15–20, https://doi.org/10.1016/j.ceb.2016.01.007.
[37] B. Casar, I. Arozarena, V. Sanz-Moreno, A. Pinto, L. Agudo-Ibanez, R. Marais, R.E. Lewis, M.T. Berciano, P. Crespo, Mol. Cell. Biol. 29 (2009) 1338–1353, https://doi.org/10.1128/MCB.01359-08.
[38] R. Kral, A. Doriguzzi, C.E. Mayer, D. Krenbek, U. Setinek, H. Sutterluty-Fall, J. Cell. Biochem. (2016), https://doi.org/10.1002/jcb.25482.
[39] J. DaSilva, L. Xu, H.J. Kim, W.T. Miller, D. Bar-Sagi, Mol. Cell. Biol. 26 (2006) 1898–1907.
[40] H. Sutterluty, E. Chatelain, A. Marti, C. Wirbelauer, M. Senften, U. Muller, W. Krek, Nat. Cell Biol. 1 (1999) 207–214.
[41] R.M. Kral, C.E. Mayer, V. Vanas, A. Gsur, H. Sutterluty-Fall, Cell Biochem. Funct. 32 (2014) 96–100.
[42] J. Lim, E.S. Wong, S.H. Ong, P. Yusoff, B.C. Low, G.R. Guy, J. Biol. Chem. 275 (2000) 32837–32845, https://doi.org/10.1074/jbc.M002156200.
[43] J.M. Mason, D.J. Morrison, B. Bassit, M. Dimri, H. Band, J.D. Licht, I. Gross, Mol. Biol. Cell 15 (2004) 2176–2188, https://doi.org/10.1091/mbc.e03-07-0503.
[44] I. Michailovici, H.A. Harrington, H.H. Azogui, Y. Yahalom-Ronen, A. Plotnikov, S. Ching, M.P. Stumpf, O.D. Klein, R. Seger, E. Tzahor, Development. 141 (2014) 2611–2620, https://doi.org/10.1242/dev.107078.
[45] E.K. Kim, E.J. Choi, Biochim. Biophys. Acta 1802 (2010) 396–405, https://doi.org/10.1016/j.bbadis.2009.12.009.
[46] G.R. Guy, R.A. Jackson, P. Yusoff, S.Y. Chow, J. Endocrinol. 203 (2009) 191–202.
[47] X. Wu, P.B. Alexander, Y. He, M. Kikkawa, P.D. Vogel, S.L. McKnight, Proc. Natl. Acad. Sci. U. S. A. 102 (2005) 14058–14062, https://doi.org/10.1073/pnas.0506714102.
[48] H.J. Kim, L.J. Taylor, D. Bar-Sagi, Curr. Biol. 17 (2007) 455–461, https://doi.org/10.1016/j.cub.2007.01.059.
[49] G.N. Medina, L.S. Ehrlich, M.H. Chen, M.B. Khan, M.D. Powell, C.A. Carter, J. Virol. 85 (2011) 7353–7362, https://doi.org/10.1128/JVI.00141-11.
[50] B. Casar, J. Rodriguez, G. Gibor, R. Seger, P. Crespo, Biochem. J. 441 (2012) 571–578, https://doi.org/10.1042/BJ20110870.
[51] D.H. Lao, P. Yusoff, S. Chandramouli, R.J. Philp, C.W. Fong, R.A. Jackson, T.Y. Saw, C.Y. Yu, G.R. Guy, J. Biol. Chem. 282 (2007) 9117–9126.
[52] A.M. Walsh, G.S. Kapoor, J.M. Buonato, L.K. Mathew, Y. Bi, R.V. Davuluri, M. Martinez-Lage, M.C. Simon, D.M. O'Rourke, M.J. Lazzara, Mol. Cancer Res. 13 (2015) 1227–1237, https://doi.org/10.1158/1541-7786.MCR-14-0183-T.
[53] P.M. Lievens, E. Zanolli, S. Garofalo, E. Liboi, FEBS Lett. 583 (2009) 3254–3258, https://doi.org/10.1016/j.febslet.2009.09.021.